

Research Article

Anti-Müllerian hormone is a survival factor and promotes the growth of rhesus macaque preantral follicles during matrix-free culture[†]

Jing Xu^{1,2,*}, Fuhua Xu², Maralee S Lawson¹, Olena Y Tkachenko¹, Alison Y Ting¹, Christoph A Kahl³, Byung S Park⁴, Richard R Stouffer¹ and Cecily V Bishop¹

¹Division of Reproductive & Developmental Sciences, Oregon National Primate Research Center, Oregon Health & Science University, Beaverton, Oregon, USA; ²Division of Reproductive Endocrinology, Department of Obstetrics & Gynecology, School of Medicine, Oregon Health & Science University, Portland, Oregon, USA; ³Molecular Virology Support Core, Oregon National Primate Research Center, Oregon Health & Science University, Beaverton, Oregon, USA and ⁴Oregon Health & Science University-Portland State University School of Public Health, Oregon Health & Science University, Portland, Oregon, USA

***Cosrrespondence:** Division of Reproductive & Developmental Sciences, Oregon National Primate Research Center, Oregon Health & Science University, 505 NW 185th Avenue, Beaverton, OR 97006, USA. Tel: +1-503-346-5411; Fax: +1-503-690-5563; E-mail: xujin@ohsu.edu

[†]**Grant support:** This research was supported by the National Institutes of Health (NIH) Eunice Kennedy Shriver National Institute of Child Health & Human Development (NICHD) R01HD082208, NIH Office of Research on Women's Health/NICHD K12HD043488 (Building Interdisciplinary Research Careers in Women's Health, BIRCWH), NIH Office of the Director P51OD011092 (Oregon National Primate Research Center Pilot Grant), and NIH/NICHD P50 HD071836 (National Center for Translational Research in Reproduction and Infertility, NCTRI). The content is solely the responsibility of the authors and does not necessarily represent the official views of the NIH.

Conference Presentation: Presented in part at the 49th Annual Meeting of the Society for the Study of Reproduction, 16–20 July 2016, San Diego, California.

Edited by Dr. Melissa E. Pepling, PhD, Syracuse University.

Received 25 June 2017; Revised 20 August 2017; Accepted 22 December 2017

Abstract

Anti-Müllerian hormone (AMH) plays a key role during ovarian follicular development, with local actions associated with a dynamic secretion profile by growing follicles. While results for AMH effects on antral follicle growth and function are consistent among studies in various species, any effects on preantral follicle development remain controversial. Therefore, experiments were conducted to investigate the direct actions and role of AMH during follicle development at the preantral stage. Macaque-specific short-hairpin RNAs (shRNAs) targeting *AMH* mRNA were incorporated into adenoviral vectors to decrease *AMH* gene expression in rhesus macaque follicles. Secondary follicles were isolated from adult macaque ovaries and cultured individually in the ultra-low-attachment dish containing defined medium supplemented with follicle-stimulating hormone and insulin for 5 weeks. Follicles were randomly assigned to treatment groups: (a) control, (b) nontargeting control shRNA-vector, (c) *AMH* shRNA-vector, (d) *AMH* shRNA-vector + recombinant human AMH, and (e) recombinant human AMH. Follicle survival and growth were assessed. Culture media were analyzed for steroid hormone and paracrine factor concentrations. For in vivo study, the nontargeting control shRNA-vector and *AMH* shRNA-vector were injected into macaque

ovaries. Ovaries were collected 9 days postinjection for morphology and immunohistochemistry assessment. Decreased *AMH* expression reduced preantral follicle survival and growth in nonhuman primates. Supplemental *AMH* treatment in the culture media promoted preantral follicle growth to the small antral stage in vitro with increased steroid hormone and paracrine factor production, as well as oocyte maturation. These data demonstrate that *AMH* is a critical follicular paracrine/autocrine factor positively impacting preantral follicle survival and growth in primates.

Summary Sentence

Anti-Müllerian hormone is a survival factor for preantral follicles in nonhuman primates, and promotes preantral follicle growth to the small antral stage with increased steroid hormone and paracrine factor production, as well as oocyte maturation.

Key words: anti-Müllerian hormone, follicle, ovary, primate, follicle culture.

Introduction

Anti-Müllerian hormone (*AMH*; previously known as Müllerian inhibiting substance), dynamically produced by developing ovarian follicles, plays a role in intraovarian regulation of folliculogenesis in adult female mammals [1]. Coexpression of *AMH* and its specific type II receptor in the granulosa cells of growing follicles indicates an autocrine and paracrine nature of the *AMH* signaling during follicular development in the ovary [2, 3]. In primate species, local actions of *AMH* to regulate follicle growth and function appear to be stage-dependent. During the initial development from the preantral to the antral stage, when follicular *AMH* production elevates along with the increase in follicle sizes [3], *AMH* is suggested to be stimulatory in promoting follicle growth in nonhuman primates and humans [4, 5]. Subsequently, *AMH* becomes inhibitory to suppress the subsequent maturation of antral follicles by limiting follicular function including steroidogenesis [4, 6]. A reduction in *AMH* production, as observed in antral follicles when they increase in size [7], could be crucial for continued antral follicle development and dominant follicle selection in primates [4].

Direct actions of *AMH* on follicular development were investigated in vitro using ovarian tissue or individual follicle culture in various species [4, 5, 8, 9]. Purified or recombinant *AMH* protein is commonly added to the culture media at a single concentration over the entire culture period. Because growing follicles produce *AMH* in gradually increasing concentrations from the preantral to the antral stage in vitro in nonhuman primates and humans [3, 10], investigation regarding the direct actions of *AMH* on follicle growth and function could be limited by endogenous *AMH* production which restricts any further effects of exogenous *AMH* treatment. In addition, the physiological role of *AMH* during folliculogenesis was studied in vivo in nonprimate species via intraperitoneal injection of recombinant *AMH* protein or *AMH* transgene-viral vector [11, 12], and in *AMH* knockout or *AMH* immunized animal models [8, 13]. Recent evidence indicates that the *AMH*-specific type II receptor is expressed by neurons in the mouse and human brain, including gonadotropin-releasing hormone neurons in the hypothalamus [14]. These systemic manipulations may not be able to discern local *AMH* actions within the ovary apart from endocrine *AMH* regulation via the hypothalamic-pituitary-ovarian axis.

Previously, an alginate-encapsulated three-dimensional culture system was established to support primate preantral follicle growth to the small antral stage, thus permitting follicular steroidogenesis, autocrine/paracrine factor production, and oocyte maturation to be monitored in vitro [15]. This follicle culture system offers a unique tool to manipulate molecular signaling pathways and related factors to obtain knowledge of their roles on follicular development in intact individual follicles. In addition, adenoviral vectors driving

constitutive expression of short-hairpin RNAs (*shRNAs*) successfully knocked down gene expression in vitro in cultured granulosa cells and in vivo via intrafollicular injection in nonhuman primates [16]. In order to apply gene knockdown approach to cultured follicles, the pore size of encapsulation material needs to be carefully considered, because it determines the diffusion efficiency of treatment agents which is more critical for adenoviral vectors with relative large diameters of 70–100 nm [17]. Although alginate matrix has been extensively researched using various techniques, its actual pore sizes remain controversial [18]. In case of alginate matrix as a barrier for viral penetration, a matrix-free system will need to be adapted for the primate follicle culture [19]. Therefore, the present study was designed to develop a molecular tool for manipulating *AMH* gene expression in the primate follicle in vitro and locally in the ovary in vivo. Experiments were also performed to examine the direct actions and role of *AMH* in the development and function of primate follicles from the secondary to the small antral stage during three-dimensional culture.

Materials and methods

Animal use

The general care and housing of rhesus macaques (*Macaca mulatta*) was provided by the Division of Comparative Medicine, Oregon National Primate Research Center (ONPRC), Oregon Health & Science University as previously described [4]. Briefly, monkeys were pair-caged in a temperature-controlled (22°C), light-regulated (12L:12D) room. Diet consisted of Purina monkey chow (Ralston-Purina) twice a day supplemented with fresh fruit or vegetables once a day and water ad libitum. Animals were treated according to the National Institutes of Health's Guide for the Care and Use of Laboratory Animals. Protocols were approved by the ONPRC Institutional Animal Care and Use Committee.

AMH knockdown by *shRNA*/small interfering RNA

RNA interference

A specific small interfering RNA (*siRNA*) complementary to the rhesus macaque *AMH* gene (NCBI gene ID 717539), targeting transcript (NCBI reference sequence XM.002801459), was designed using BLOCK-iT RNAi Designer (Life Technologies; Table 1). A scrambled *siRNA* was designed to serve as a nontargeting control (NTC; Table 1). Sequences were encoded within Stealth RNAi *siRNAs* (Life Technologies) and evaluated for their ability to deplete *AMH* mRNA expression in Sertoli cells. Testes were collected from three male macaque fetuses at necropsy (130 days gestation). Cesarean section and euthanasia were performed by the Surgical

Table 1. Short-interfering RNAs and shRNAs used for *AMH* knockdown study.

Oligo	Type	Nucleotide sequence (5' to 3')
siAMH.Top	siRNA_top sequence	CCUUGCGAGCUCUGCUGCUUCUGAA
siAMH.Bottom	siRNA_bottom sequence	UUCAGAAGCAGCAGAGCUCGCAAGG
siScram.Top	siRNA_top sequence	CCUGCGAUCUCCGGUCCUUGUGAA
siScram.Bottom	siRNA_bottom sequence	UUCACAAGGAACCGGAGAUCCGAGG
shAMH.Top	shRNA_top sequence	CACCGCCTTGCAGCTCTGCTGCTTCTGAACGAATTCAGAAGCAGCAGAGCTCGCAAGG
shAMH.Bottom	shRNA_bottom sequence	AAAACCTTGCAGCTCTGCTGCTTCTGAATTCGTTTCAAGAAGCAGCAGAGCTCGCAAGGC
shScram.Top	shRNA_top sequence	CACCGCCTTGCAGCTCTCGGTTCCCTTGTGAACGAATTCACAAGGAACCGGAGATCGCAGG
shScram.Bottom	shRNA_bottom sequence	AAAACCTTGCAGCTCTCGGTTCCCTTGTGAATTCGTTTCAAGAAGGAACCGGAGATCGCAGGC

Services Unit and the Pathology Services Unit at ONPRC for research projects unrelated to the current study. Sertoli cells were isolated and cultured as previously reported [20]. Cells from each animal were divided to four groups for 24-h incubation according to the Oligofectamine protocol from the manufacturer: (a) control media only, (b) entry vector plasmid (for shRNA cloning; Life Technologies), (c) NTC siRNA, and (d) *AMH* siRNA. Cells were subsequently cultured for 4 days and harvested for RNA extraction. RNA was reverse-transcribed to cDNA for real-time PCR evaluation on *AMH* expression as previously reported [3]. The validated siRNA sequences were then expanded into longer shRNAs that included either NTC siRNA or *AMH* siRNA (Table 1). The shRNAs were cloned into the entry vector plasmid for incorporation into the viral vectors by the Molecular Virology Support Core at ONPRC as previously described [16].

Adenoviral vector generation and validation

Adenoviral vectors expressing shRNA targeting *AMH* mRNA, NTC shRNA, or the gene encoding enhanced green fluorescent protein (*EGFP*) via cytomegalovirus promoter were constructed using the ViraPower system (Life Technologies) as previously reported [16]. During pilot studies, the *EGFP* gene-expressing vector (*EGFP*-vector) was used to determine the optimal viral titer for sufficient transduction of granulosa cells in macaque follicles developed in vitro, and to ensure high *EGFP* expression and low toxicity by comparing follicle survival rates between the viral vector-treated and the media-only control cultures.

For encapsulated three-dimensional follicle culture, ovaries were collected from three animals (12–13 year old) at necropsy by the Pathology Services Unit, ONPRC. Euthanasia was due to reasons unrelated to reproductive health. The process of follicle isolation, encapsulation, and culture was reported previously [4]. Briefly, secondary follicles (diameter 125–225 μm) were mechanically isolated, encapsulated individually in 0.25% (w/v) sodium alginate gel matrix (FMC BioPolymers)-phosphate-buffered saline (PBS; 137 mM NaCl, 10 mM phosphate, 2.7 mM KCl; Thermo Fisher Scientific Inc.), and cultured in 300 μl media in 48-well plates at 37°C and 5% O₂. Culture media contained alpha minimum essential medium (Thermo Fisher Scientific Inc.) supplemented with 1 ng/ml recombinant human follicle-stimulating hormone (NV Organon), 6% (v/v) human serum protein supplement (Cooper Surgical, Inc.), 0.5 mg/ml bovine fetuin, 5 $\mu\text{g}/\text{ml}$ insulin, 5 $\mu\text{g}/\text{ml}$ transferrin, 5 ng/ml sodium selenite, and 10 $\mu\text{g}/\text{ml}$ gentamicin (Sigma-Aldrich). Secondary follicles from each of the three animals were randomly assigned to culture groups (12 follicles/monkey/group) with either control media only or 24-h *EGFP*-vector exposure at a range of 9.6×10^5 – 9.6×10^7 plaque-forming units (pfu)/ml. Media (150 μl) was changed every other day starting from culture day 2. Fluorescence microscopy was performed 24 h and 7 days post-viral exposure using an Olympus

Inverted System microscope (IX71; Olympus Imaging America Inc.) attached to a reflected light fluorescence laser with filter to identify fluorescein isothiocyanate emission spectra as previously described [16].

In order to develop a matrix-free three-dimensional system to achieve efficient diffusion of viral vectors and macromolecules during macaque follicle culture, ovaries were collected from four animals (12–13 year old) at necropsy. Isolated secondary follicles from each of the four animals were either encapsulated with alginate matrix for culture in the control media as described above, or distributed individually into wells of the 96-well ultra-low attachment microplates (Corning Inc.) for matrix-free culture with 200 μl control media (6–24 follicles/monkey/group) at 37°C and 5% CO₂. Media, 150 μl for encapsulated culture and 100 μl for matrix-free culture, was changed every other day during 5 weeks of culture. Follicle survival (percentage of surviving follicles versus total follicles cultured), antrum formation (percentage of antral follicles versus total follicles survived), and growth (follicle diameter) were assessed weekly by microscopy as previously described [4]. Follicle diameters were measured using Image J 1.50 software (National Institutes of Health).

To examine the adenoviral vector transduction in macaque follicles during the matrix-free culture, ovaries were collected from three animals (12–13 year old) at necropsy as described above. Isolated secondary follicles from each of the three animals were randomly assigned to treatment groups (12 follicles/monkey/group) for the matrix-free culture as described above, with either control media only or 24-h *EGFP*-vector exposure at a range of 9.6×10^5 – 9.6×10^7 pfu/ml. Media (100 μl) was changed every other day starting from culture day 2. Fluorescence microscopy was performed 24 h post-viral exposure as described above. On culture day 7, selected follicles were fixed individually in 4% paraformaldehyde-PBS solution, embedded in paraffin, and sectioned by the Imaging and Morphology Support Core at ONPRC for immunohistochemistry (IHC) staining using rabbit anti-GFP antibody (1:500; ab290; Abcam) with nuclear fast-red counterstain (Sigma-Aldrich) as previously reported (Supplementary Table S1) [15, 16]. Following incubation of alkaline phosphate-conjugated secondary antibody, the EGFP staining in the follicle was detected with application of NBT/BCIP substrate (Roche) [16]. The expression of *EGFP* transgene in cultured follicles was also visualized using a Leica SP5 confocal-equipped DM6000 CFS microscope (Leica Microsystems Inc.) at day 7 post-viral exposure as described previously [21]. Culture was extended to 5 weeks to determine toxic effects of adenovirus exposure on cultured follicles.

In vitro study

Follicle culture

Ovaries were collected from three animals (7–13 year old) at necropsy. Isolated secondary follicles (diameter = 140–225 μm)

from each of the three animals were randomly assigned to five groups (15 follicles/monkey/group) for 5 weeks of matrix-free culture as described above: (a) control media-only, (b) 9.6×10^5 pfu/ml NTC shRNA-vector incubation for 24 h, (c) 9.6×10^5 pfu/ml *AMH* shRNA-vector incubation for 24 h, (d) 9.6×10^5 pfu/ml *AMH* shRNA-vector incubation for 24 h + 100 ng/ml recombinant human AMH (rhAMH; 1737-MS; disulfide-linked C-terminal homodimer; R&D Systems, Inc.; based on a preliminary dose-response study using 50 and 100 ng/ml rhAMH) during culture weeks 0–2 (exogenous AMH replacement before antrum formation following endogenous AMH depletion) [4], and (e) 100 ng/ml rhAMH during culture weeks 0–2. Media (100 μ l) was changed every other day starting from culture day 2. Follicle survival, antrum formation, and growth were assessed weekly as described above.

Ovarian steroid and paracrine factor assays

In order to assess steroidogenic function in cultured follicles, media samples were analyzed for estradiol (E2) and progesterone (P4) concentrations using a chemiluminescence-based automatic clinical platform (Immolute 2000; Siemens Healthcare Diagnostics), and androstenedione (A4) concentrations using enzyme-linked immunosorbent assay (ELISA; AA E-1000 kit; Rocky Mountain Diagnostics, Inc.), which were validated for macaque serum and follicle culture media, by the Endocrine Technology Support Core at ONPRC as reported previously [4].

In order to assess follicular function in paracrine factor production during culture, media samples were also assayed by ELISA for concentrations of AMH using an SKU: AL-105 kit (AnshLabs) [3] and vascular endothelial growth factor (VEGF) using a Human VEGF Quantikine ELISA Kit (R&D Systems, Inc.) [15] based on the manufacturers' instructions, which were validated previously for macaque serum and follicle culture media. Media activin A concentrations were assayed using an Activin A ELISA Kit (SKU: AL-110; AnshLabs) based on the manufacturer's instructions. The assay was validated for parallelism with blank culture media containing a known concentration of activin A, and with media used in culture with macaque follicles. The sensitivity of the assay was 40 pg/ml for 25 μ l sample. The standard curve of the assay ranged 40–1000 pg/ml.

Oocyte maturation and fertilization

Oocyte maturation and fertilization *in vitro*, as well as the subsequent embryo culture, were reported previously [4]. Briefly, at the end of culture week 5, antral follicles were treated with 100 ng/ml recombinant human chorionic gonadotropin (hCG; Merck Serono) for 34 h before harvesting the enclosed oocyte for diameter measurement and meiotic status assessment via microscopy. Metaphase II (MII) oocytes were inseminated via conventional *in vitro* fertilization. Fertilization was confirmed by the presence of two polar bodies and two pronuclei 16 h post-*in vitro* fertilization. Zygotes were cultured in 100 μ l Global Medium (LifeGlobal Group) containing 10% (v/v) fetal bovine serum at 37°C in 5% O₂/6% CO₂/89% N₂ according to protocols provided by the Assisted Reproductive Technologies Support Core at ONPRC.

In vivo study

Intraovarian injection

Three monkeys exhibiting regular menstrual cycles, with the first day of menstruation considered day 1 of the cycle, were assigned to the study. On day 2 of the cycle (early follicular phase), 1 ml blood

sample was collected via venipuncture in the arm. Additional 1 ml blood samples were collected from the right and the left ovarian veins of anesthetized monkeys via laparotomy by the Surgical Services Unit at ONPRC, followed by intraovarian injections as reported previously [16]. Briefly, the NTC shRNA-vector and *AMH* shRNA-vector were diluted in 100 μ l PBS to 9.6×10^5 pfu/ml and drawn into a 1 ml tuberculin syringe for injection into the right and the left ovary, respectively. The needle was inserted through the stroma into the center of the ovary for injection. The needle was removed and the ovary was observed to ensure that leakage did not occur.

At day 9 postinjection, 1 ml blood sample was collected via venipuncture in the arm. Additional 1 ml blood samples were collected from the right and the left ovarian veins of anesthetized monkeys via laparotomy, followed by oophorectomy procedures to collect ovaries as reported previously [16].

AMH assay

Blood samples were assayed for serum AMH concentrations by ELISA using an SKU: AL-105 kit (AnshLabs) based on the manufacturer's instruction [3].

Ovarian histology and IHC

Ovaries were fixed in 4% paraformaldehyde-PBS solution, embedded in paraffin, and sectioned for hematoxylin and eosin staining as previously reported [15]. IHC was performed using mouse anti-human AMH antibody (1:75; MAB1737; R&D Systems, Inc.) as previously reported (Supplementary Table S1) [3]. Slides were then incubated with biotinylated anti-mouse IgG and processed using a VECTASTAIN Elite ABC Kit (PK-6102; Vector Laboratories, Inc.). Following incubation with 3,3'-diaminobenzidine, sections were counterstained using hematoxylin. Images were captured using an Olympus BX40 inverted microscope and an Olympus DP72 digital camera (Olympus Imaging America Inc.).

Selected ovarian sections were assessed for cell-cycle inhibition by IHC using rabbit anti-human cyclin-dependent kinase inhibitor 1A (p21) antibody (1:100; 2947; Cell Signaling Technology) as previously reported (Supplementary Table S1) [22]. The activation of p21 expression indicates cell cycle arrest and the inhibition of granulosa cell proliferation in macaque ovarian follicles [22]. Following secondary antibody incubation and hematoxylin counterstaining, as described above, images were captured using a Revolve microscope (Echo Laboratories).

Statistical analysis

Statistical analysis was performed using SAS V9.4 software (SAS Institute Inc.). Due to the limited sample size and uncertainty of distribution for formal statistical hypothesis testing, a permutation test (randomization test) was used to compare *AMH* mRNA levels and media activin A concentrations between groups as reported previously [4]. Due to the skewed distributions, a mixed model was used for analyses of follicle survival, growth and antrum formation rates, media steroid and VEGF concentrations, as well as serum AMH concentrations with rank-based analysis or logarithmic transformation applied. One-way ANOVA followed by the Student–Newman–Keuls post hoc test was performed to compare media AMH concentrations between groups. Differences were considered significant at $P < 0.05$ and values are presented as the mean \pm SEM.

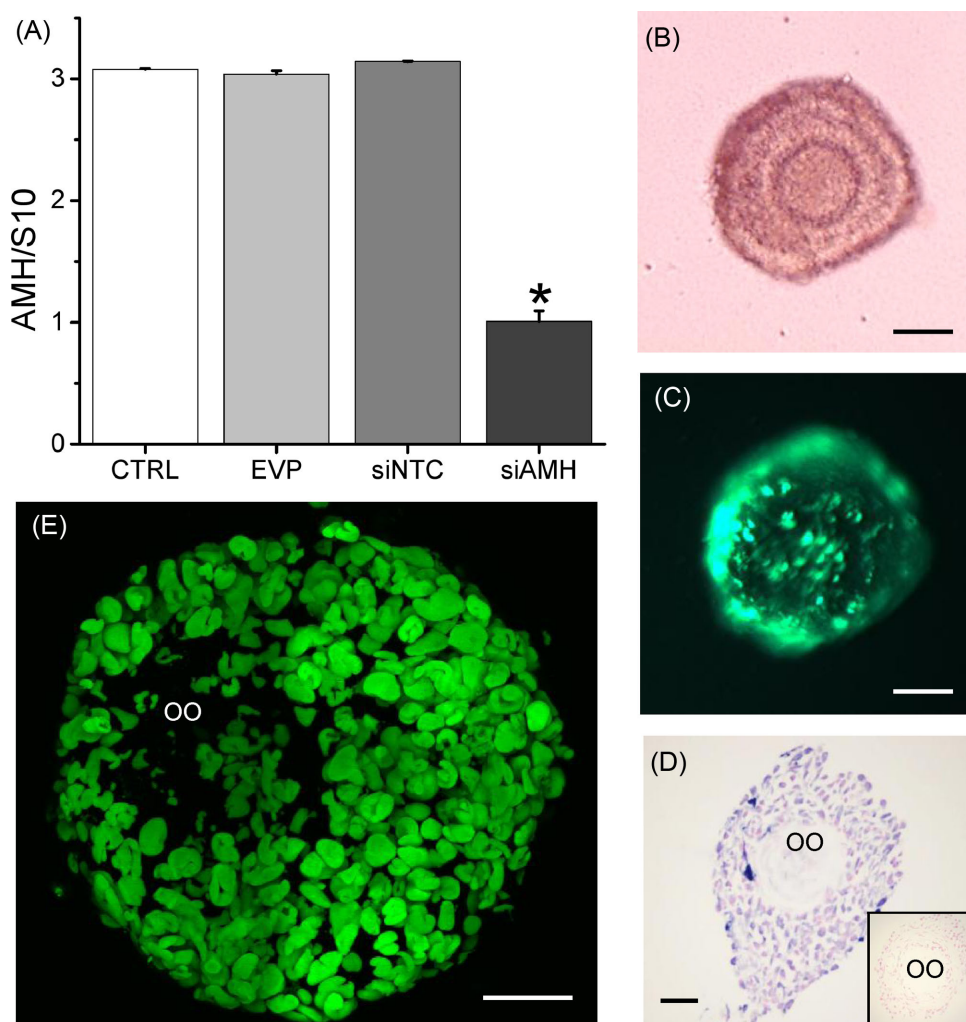


Figure 1. The validation of anti-Müllerian hormone (AMH) knockdown via small interfering RNA (siRNA) as indicated by *AMH* mRNA levels in Sertoli cells from macaque fetal testes at culture day 4 following 24 h of treatment (A; $n = 3$ animals), and the efficiency of adenoviral vector transduction in macaque secondary follicles during matrix-free three-dimensional culture (B; secondary follicle in culture) as indicated by enhanced green fluorescent protein (EGFP) expression 24 h post the *EGFP* gene-expressing vector incubation (C), as well as the EGFP immunostaining (D; blue is the positive staining and red is the counterstaining; negative control inserted) and fluorescent signal (E) at culture day 7. Data in panel A are presented as the mean \pm SEM. CTRL, control media only; EVP, entry vector plasmid (for shRNA cloning) only incubation; siNTC, nontargeting control siRNA incubation; siAMH, AMH siRNA incubation; S10, S10 RNA for internal control; OO, oocyte; *significant difference with $P < 0.05$; scale bar = 50 μm .

Results

The protocol for *AMH* knockdown in macaque follicles via adenoviral vector transduction was successfully established and validated. *AMH* siRNA, but not NTC siRNA or the entry vector plasmid, suppressed *AMH* mRNA expression by cultured Sertoli cells at culture day 4 post-treatment (Figure 1A) without any effects on cellular viability or total RNA recovered (data not shown).

No *EGFP* transgene expression was detected (absence of green fluorescence) in alginate-encapsulated follicles at any dosage of the *EGFP*-vector tested during the entire 7 days of culture. Typically, *EGFP* expression is readily apparent in granulosa cells 24 h after exposure to this *EGFP*-vector [16]. The observation suggested that the pore size of the alginate matrix did not allow the diffusion of adenoviral vectors.

At week 5, the survival rates, antrum formation rates, diameters and media E2 concentrations were not statistically different between follicles developed in alginate-encapsulated and matrix-free cultures

($57 \pm 13\%$ versus $44 \pm 7\%$; $72 \pm 13\%$ versus $57 \pm 15\%$; $448 \pm 39 \mu\text{m}$ versus $511 \pm 32 \mu\text{m}$; and 1163 ± 536 versus $1173 \pm 463 \text{ pg/ml}$, respectively). During the matrix-free culture, the expression of *EGFP* transgene (green fluorescence) in follicles was detectable at 24 h post-viral exposure (Figure 1B and C). The positive EGFP immunostaining (Figure 1D) and expression of *EGFP* transgene (Figure 1E) was also observed in granulosa cells, but not the oocyte, of cultured follicles at day 7 post-viral exposure. At culture week 5, the survival rates were not statistically different between follicles developed in control media and with *EGFP*-vector exposure at 9.6×10^5 pfu/ml ($63 \pm 21\%$ versus $56 \pm 22\%$). The toxic effects of adenovirus exposure on cultured follicles were not observed.

In vitro study

The role of AMH during preantral follicle development was studied via adenoviral vector transduction in macaque follicles in vitro during matrix-free three-dimensional culture. Following 24 h of *AMH*

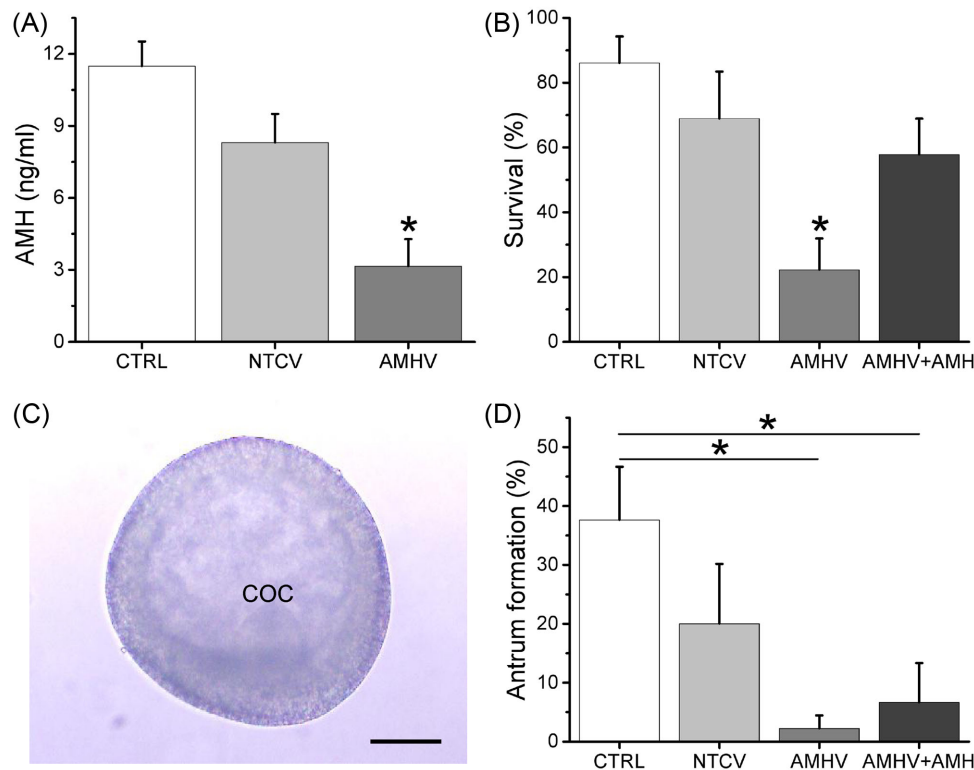


Figure 2. The effects of anti-Müllerian hormone (AMH) knockdown and AMH replacement on the AMH production by macaque secondary follicles at culture week 2 (A; $n = 10$ follicles/group), the survival rates (percentage of surviving follicles/total cultured follicles) of macaque secondary follicles at culture week 2 (B; $n = 45$ total cultured follicles/group), and, when the antrum formation occurred at culture week 3 (C), the antrum formation rates (percentage of antral follicles/total surviving follicles) of macaque follicles developed in vitro (D; $n = 10$ –37 total surviving follicles/group). Data in panels A, B, and D are presented as the mean \pm SEM. CTRL, control media only; NTCV, nontargeting control short hairpin RNA (shRNA)-vector incubation for 24 h; AMHV, AMH shRNA-vector incubation for 24 h; AMHV + AMH, AMH shRNA-vector incubation for 24 h + rhAMH addition during culture weeks 0–2; COC, cumulus-oocyte complex; *, significant difference between experimental groups with $P < 0.05$; scale bar = 100 μ m.

shRNA-vector treatment, AMH protein production by cultured secondary follicles decreased, with media AMH concentrations 73% lower ($P < 0.05$) than those of the control follicles at culture week 2 (Figure 2A). There were no differences in week 2 media AMH concentrations between the control and the NTC shRNA-vector groups (Figure 2A).

While survival rates of the secondary follicles were not statistically different between the control and the NTC shRNA-vector groups at culture week 2, AMH shRNA-vector treatment decreased ($P < 0.05$) follicle survival compared with controls (Figure 2B). The additional rhAMH treatment during the first 2 weeks of culture for the AMH shRNA-vector-treated follicles increased ($P < 0.05$) follicle survival to the control levels (Figure 2B). For surviving follicles, those that grew formed an antrum at culture week 3 (Figure 2C). While antrum formation rates of cultured follicles were not statistically different between the control and the NTC shRNA-vector groups at week 3, only 1 out of 10 surviving follicles from all animals in the AMH shRNA-vector group formed an antrum, with antrum formation rates lower ($P < 0.05$) than those of the control group (Figure 2D). The antrum formation rates stayed low ($P < 0.05$) compared with controls in the presence of rhAMH for the AMH shRNA-vector-treated follicles, which were not statistically different from those of the AMH shRNA-vector alone group (Figure 2D).

For secondary follicles cultured with rhAMH only, without the AMH shRNA-vector treatment, follicle survival rates were not

statistically different from controls at week 2 ($84 \pm 6\%$ versus $86 \pm 8\%$). Although there were no differences in diameters of secondary follicles between the control and the rhAMH groups at the beginning of culture (195 ± 5 versus $191 \pm 5 \mu$ m), diameters were larger ($P < 0.05$) for the rhAMH-treated follicles compared with those of controls at week 2 before antrum formation (Figure 3A). The antrum formation rates between the control and the rhAMH groups were not statistically different at culture week 3 ($38 \pm 9\%$ versus $53 \pm 7\%$).

Due to continued expression of shRNAs in cultured follicles after antrum formation by viral vectors, which confounded the stage-dependent AMH actions, the function of in vitro-developed small antral follicles was only analyzed in the control and rhAMH groups. Cultured follicles produced measureable amounts of steroid hormones in the media. Following antrum formation at week 3, the media E2 concentrations were higher ($P < 0.05$) in follicles treated with rhAMH for the first 2 weeks compared with controls (Figure 3B). Media A4 concentrations at culture week 3 also showed a tendency to increase ($P = 0.059$) in the rhAMH group relative to the control group (78 ± 47 versus 6 ± 4 pg/ml). There were no differences in media P4 concentrations between the control and the rhAMH group at culture week 3 (6 ± 3 versus 8 ± 5 ng/ml). Peptide factors produced by cultured follicles were also detectable in the media. Follicles treated with rhAMH during the first 2 weeks of culture produced VEGF at increased ($P < 0.05$) concentrations at week 3

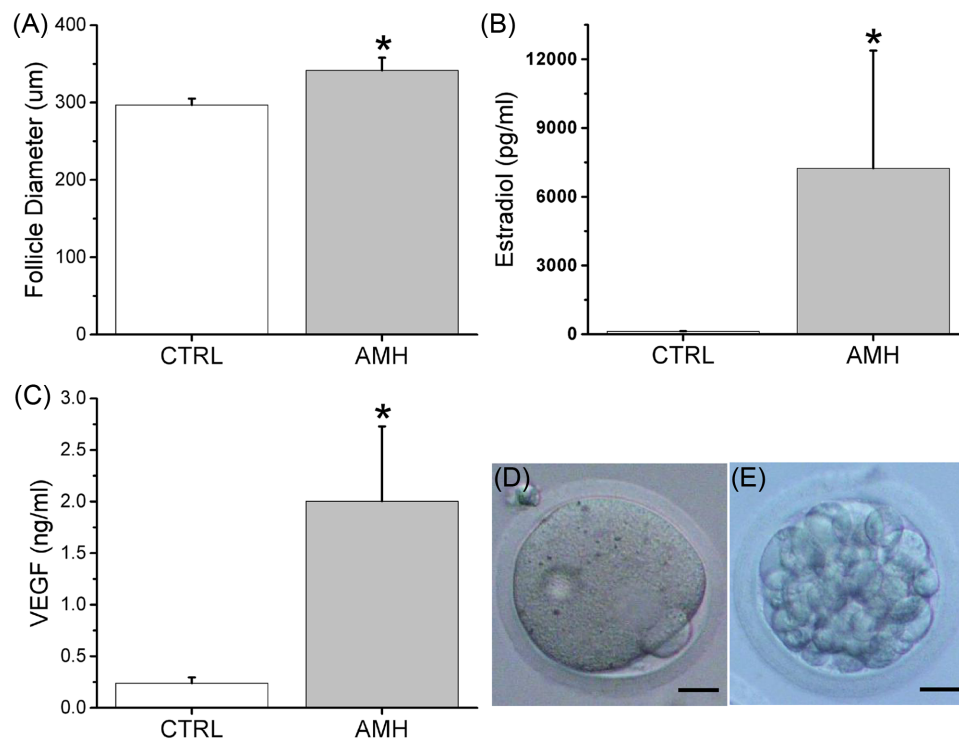


Figure 3. The effects of anti-Müllerian hormone on the macaque secondary follicle growth (follicle diameter) at culture week 2 (A; $n = 10\text{--}19$ follicles), the production (media concentration) of estradiol (B; $n = 10$ follicles) and vascular endothelial growth factor (VEGF; C; $n = 10$ follicles) by in vitro-developed macaque small antral follicles at culture week 3, and oocyte maturation in in vitro-developed macaque small antral follicles following recombinant hCG treatment at culture week 5 as represented by an metaphase II oocyte (D) which developed to the morula stage (E) when fertilized via in vitro fertilization. Data in panels A, B, and C are presented as the mean \pm SEM. CTRL, control; AMH, recombinant human anti-Müllerian hormone addition during culture weeks 0–2; *, significant difference with $P < 0.05$; scale bar = $25\ \mu\text{m}$.

Table 2. Characteristics of oocytes harvested from antral follicles at week 5 of matrix-free three-dimensional culture (34 h after addition of recombinant hCG).

Culture conditions	Follicles harvested	Oocytes obtained	Number (%) of				Diameter (μm)		
			Degenerate oocytes ^a	Healthy oocytes			GV oocytes	MI oocytes	MII Oocytes
CTRL	14	14	5 (36%)	8 (89%)	0	1	108 ± 3	–	121
rhAMH	19	19	3 (16%)	10 (63%)	4	2	112 ± 2	114 ± 2	114, 121

Values are the mean \pm SEM with each oocyte as an individual data point. CTRL, control; rhAMH, recombinant human anti-Müllerian hormone; GV, germinal vesicle; MI, metaphase I; MII, metaphase II.

^aPercentage of degenerate oocytes versus total oocytes obtained.

^bPercentage of GV oocytes versus total healthy oocytes obtained.

compared with those of the control follicles (Figure 3C). Activin A was only detectable in the media of follicles treated with rhAMH and reached a peak level of $50 \pm 5\ \text{pg/ml}$ at culture week 5.

When treated with hCG at the end of culture week 5, 64% oocytes harvested from the control group and 84% from the rhAMH group exhibited healthy morphology (Table 2). About 89% of the healthy oocytes from the control group remained at the germinal vesicle intact stage, while only one oocyte matured to the MII stage (Table 2). In the rhAMH group, 63% of the healthy oocytes remained at the germinal vesicle intact stage with diameters similar to those of the control group (Table 2). Four oocytes developed to the metaphase I stage and two to the MII stage (Figure 3D). The MII oocytes were fertilized following in vitro fertilization with the resulting embryos developed to the morula stage (Figure 3E).

In vivo study

The role of AMH in developing preantral follicles was also studied via adenoviral vector transduction in macaque ovaries in vivo using intraovarian injection technique. In the NTC shRNA-vector-treated ovary (right ovary), AMH immunostaining was undetectable in primordial follicles, but was evident in granulosa cells of the preantral (primary and secondary) follicles and became intense in small antral follicles 9 days postinjection (Figure 4A). At day 9 post-AMH shRNA-vector injection, AMH immunostaining in the ovary (left ovary) was diminished in both the preantral (primary and secondary) and small antral follicles (Figure 4B). Immunostaining for AMH remained undetectable in primordial follicles following AMH shRNA-vector injection (Figure 4B). At day 9 postinjection, serum AMH concentrations in the right ovarian vein, which was connected to the

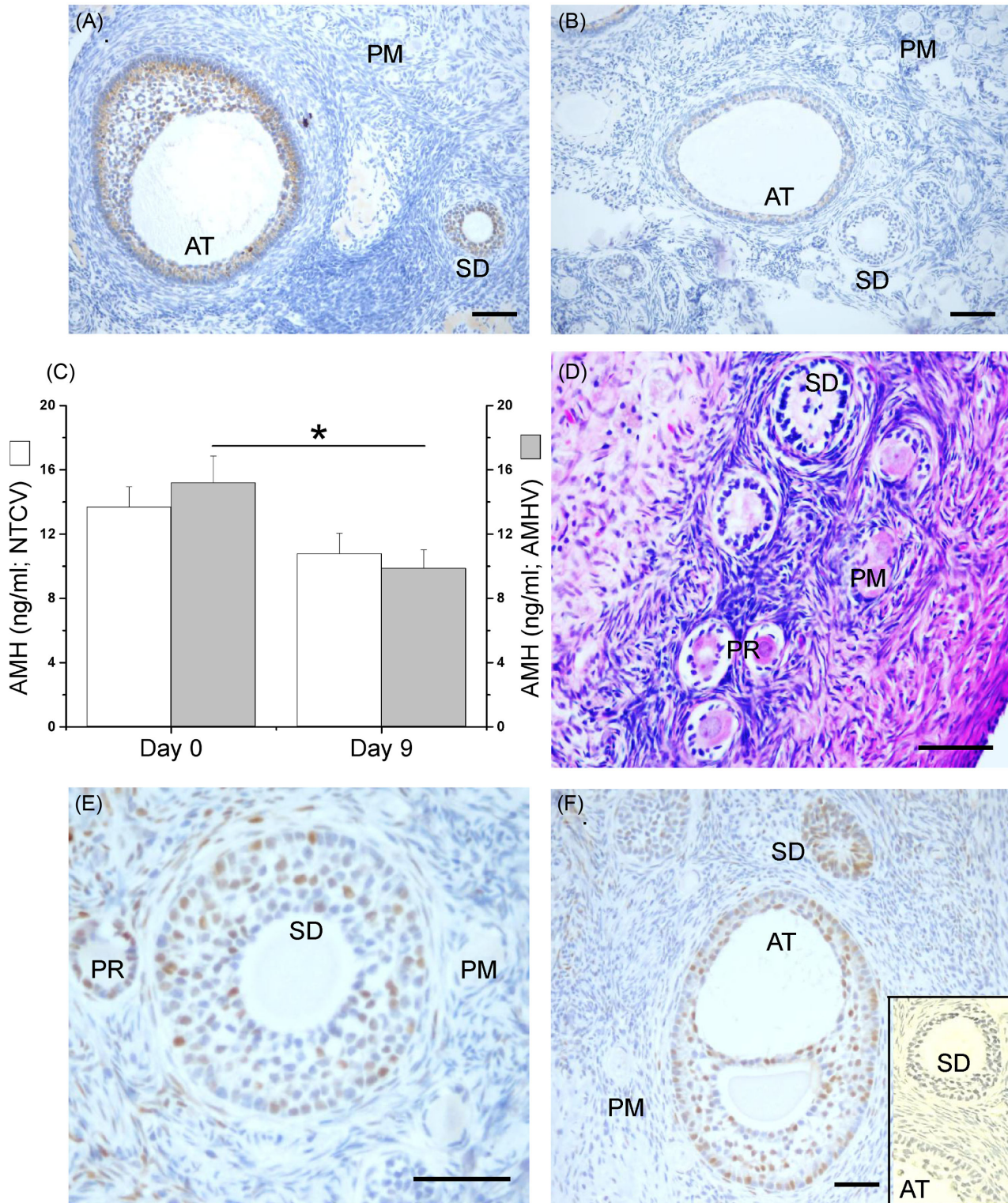


Figure 4. The effects of local anti-Müllerian hormone (AMH) knockdown in the macaque ovary 9 days post a signal intraovarian injection of short-hairpin RNA (shRNA) vectors as presented by the AMH immunostaining in the ovary injected with the nontargeting control (NTC) shRNA-vector (right ovary; brown is the positive staining and blue is the counterstaining; A) or the *AMH* shRNA-vector (left ovary; B), the serum AMH concentrations from the right and the left ovarian veins prior to injection (day 0) and 9 days postinjection (C; $n = 3$ animals), the hematoxylin and eosin staining of the ovary injected with the *AMH* shRNA-vector (D), and the p21 (cyclin-dependent kinase inhibitor 1A) immunostaining in the ovary injected with the *AMH* shRNA-vector (brown is the positive staining and blue is the counterstaining; E and F) or NTC shRNA-vector (F inset). Data in panel C are presented as the mean \pm SEM. NTCV, NTC shRNA-vector injection; AMHV, *AMH* shRNA-vector injection; PM, primordial follicle; PR, primary follicle; SD, secondary follicle; AT, small antral follicle; *, significant difference with $P < 0.05$; scale bar = 100 μ m.

ovary treated with the NTC shRNA-vector, were not statistically different from those measured in the same vein prior to the injection (Figure 4C). However, serum AMH concentrations in the left ovarian vein, which was connected to the ovary treated with *AMH* shRNA-vector, were lower ($P < 0.05$) at day 9 postinjection than those measured from the same vein prior to the injection (Figure 4C). Serum AMH concentrations collected from peripheral veins were not significantly different between samples collected before the injection and 9 days postinjection (17 ± 2 versus 14 ± 1 ng/ml).

At day 9 postinjection, primordial and preantral follicles of ovaries injected with the NTC shRNA-vector exhibited normal healthy morphology typically observed in macaque ovaries (data not shown). While there were no morphologic abnormalities observed in primordial follicles of ovaries injected with the *AMH* shRNA-vector, abnormal morphology of preantral (primary and secondary) follicles was readily apparent including disorganized granulosa cells, condensed or vacuolated oocytes, and an evident disassociation between the basement membrane of follicles and the surrounding stroma (Figure 4D). Immunostaining of p21 was abundantly detected in granulosa cells of preantral (primary and secondary) and small antral follicles in the *AMH* shRNA-vector-injected ovaries (Figure 4E and F). Very few p21-positive granulosa cells were detected in both the preantral (primary and secondary) and small antral follicles in ovaries injected with the NTC shRNA-vector (Figure 4F, inset). No p21-positive staining was evident in primordial follicles in ovaries of any treatment groups.

Discussion

In the current study, we investigated the physiological role of AMH during preantral follicle development, employing adenoviral vector-mediated shRNA/siRNA silencing of *AMH* gene in the developing follicle of nonhuman primates. For the first time, the manipulation of *AMH* gene expression was achieved in individual follicles in vitro using three-dimensional culture, and locally in the ovary in vivo via intraovarian injection. These data provide the first in vitro and in vivo evidence to suggest that AMH acts as a survival factor in the nonhuman primate ovarian follicle at the preantral stage. The in vitro data further support the hypothesis that locally produced AMH plays a stimulatory role during primate preantral follicle development.

Endogenous *AMH* expression was successfully knocked down in granulosa cells of macaque preantral follicles developing in vitro. Pilot studies employing an adenoviral vector-mediated transduction of *EGFP* transgene demonstrated that the adenoviral vector failed to transduce cells of alginate-encapsulated follicles, suggesting that the pore size of 0.25% (w/v) alginate matrix was less than 70 nm, the minimum diameter of adenoviruses [17]. This obstacle was overcome by adapting a matrix-free three-dimensional culture system that achieved similar outcomes of primate follicular development in vitro. The data from macaque follicles are consistent with a previous study demonstrating that mouse preantral follicles cultured in ultra-low attachment microplates survived and grew to the antral stage with correlated steroid production and oocyte maturation [19]. In the current study, the adenoviral vector-driving expression of shRNA, which was processed within the cell to the specific siRNA, was able to transduce granulosa cells within 24 h of incubation, with continued expression of shRNA in multiple granulosa layers 6 days postexposure as demonstrated by *EGFP* transgene expression. The decrease in follicular AMH protein secretion extended to 2 weeks, which covered the entire preantral span of primate follicles developed in vitro. Notably, the oocyte was not transduced, indicating

that the adenoviral vector could not penetrate the zona pellucida, and thus, did not affect oocyte gene expression. This model provides a tool to study the function of follicular cell-specific genes and the impact of macromolecules in intact follicles during specific (preantral and/or antral) stages of in vitro development.

Knockdown of *AMH* gene expression by adenoviral vector-mediated transduction was also efficient in vivo. Following a single intraovarian injection of *AMH* shRNA-vector, AMH protein expression by granulosa cells stayed low in both the preantral and small antral follicles in the ovary up to 9 days postinjection, as demonstrated by limited AMH immunostaining density and reduced serum AMH levels in the connected ovarian vein. The data are consistent with a study in which transduction activity lasted weeks in vivo following a single intraovarian injection of adenoviral vector-mediated transgene in mice [23]. In the same study, multiple organ samples were collected postinjection to evaluate the safety and toxicity of direct intraovarian inoculation of adenoviral vectors. Adenoviral-specific DNA was only detected in the injected ovary and the adjacent oviduct, but not the contralateral ovary or other organs [23]. This evidence supports our observation that the contralateral ovary injected with the NTC shRNA-vector maintained its AMH production in granulosa cells of the preantral and small antral follicles. The circulating levels of AMH were not significantly altered by *AMH* knockdown in one of the two ovaries, which avoided any systemic effects via alterations in binding and activation of the AMH-specific type II receptor in multiple brain regions including the hypothalamus [14]. Therefore, this model provides a tool to study the function of follicular cell-specific genes employing local manipulation of gene expression in the ovary in vivo.

Knocking down *AMH* expression in macaque preantral follicles negatively impacted follicle survival as demonstrated by the reduced survival rates in vitro following *AMH* shRNA-vector exposure, which was recovered by AMH protein replacement, and by the abnormal morphology associated with follicular atresia in vivo following *AMH* shRNA-vector inoculation in the ovary. The data are consistent with the previous study in which AMH treatment enhanced the survival of small growing follicles in cultured human ovarian cortex [5]. Mice heterozygous for the *Amb* null mutation also revealed an increased number of atretic small follicles within their ovaries, which became more significant in the *Amb* null mice, compared with wild types [24]. However, this positive effect of AMH on preantral follicle survival was not observed in either the current study or in other studies employing follicle culture in mice [8] and nonhuman primates [4] by simply administering a consistent dose of AMH protein to the culture media. The limited exogenous AMH actions may be due to the increased endogenous AMH production by the growing follicles and/or the already high survival rates of individually cultured follicles under the control conditions. Previous research indicated that AMH treatment reduced apoptosis of follicles in the cryopreserved mouse ovary in a dose-dependent manner [25]. Therefore, AMH may act as a survival factor in preantral follicles via its antiapoptotic actions to prevent follicular atresia. Studies are warranted to further corroborate the mechanisms of programmed cell death in follicles that are related to AMH signaling, including apoptosis, autophagy, and necroptosis. Notably, primordial follicle atresia was not evident following *AMH* knockdown in vivo in the current study. Since neither *AMH* nor AMH specific type II receptor is expressed in primordial follicles, as suggested by in situ hybridization in the rat ovary [2] and by IHC in the macaque ovary [3], AMH may not play a major role in primordial follicles via direct actions in adult animals.

Knocking down *AMH* expression in macaque preantral follicles also negatively impacted follicle growth as demonstrated by the reduced antrum formation in vitro following *AMH* shRNA-vector exposure and by the increased granulosa cell p21 expression in vivo following *AMH* shRNA-vector inoculation in the ovary. The activation of p21 expression sustains cell cycle arrest, which prohibits cell proliferation [26]. The data are consistent with the previous study in which vitrification of human ovarian tissue down-regulated *AMH* mRNA levels in granulosa cells of preantral follicles, compared with those of fresh control tissue by single-cell mRNA analysis, with delayed growth during the subsequent follicle culture [27]. Interestingly, the detained follicle growth caused by *AMH* knockdown was not significantly improved by *AMH* protein replacement in the current study, which warrants further investigation via a dose-response experiment. Nevertheless, addition of rhAMH alone during the preantral stage promoted follicle growth in vitro as indicated by increased follicle diameters relative to controls. It appeared that the advanced granulosa cell proliferation and follicle growth proceeded to the early antral stage with correlated ovarian steroid (E2 and A4) and paracrine factor (VEGF and activin A) production, as well as oocyte maturation. The data support the previous notions that AMH promoted the growth of preantral follicles in rats during the serum-free culture [28], in macaques during the alginate-encapsulated three-dimensional culture [4], and in humans during the ovarian cortex culture [5]. Therefore, it is suggested that AMH plays a stimulatory role during preantral follicle development in vitro by promoting granulosa cell proliferation.

An rhAMH protein used in this study is a disulfide-linked C-terminal homodimer. Endogenously, AMH is synthesized as the propeptide precursor and is processed into the mature C-terminal dimer. The proregion remains associated with the mature ligand in a noncovalent complex after proteolytic cleavage. Proregion dissociation generates mature ligand, which contributes to the assembly of a fully active receptor complex, though dissociation of the proregion from the mature C-terminal dimer is not required for the initial interaction with the receptor complex [29]. Previous research indicated that binding affinity of the noncovalent complex and the C-terminal dimer for specific AMH receptor II appeared to be similar. The mature C-terminal dimer was more active than the noncovalent complex in stimulating downstream SMAD phosphorylation, which suggested that the proregion attenuated the activity of the C-terminal dimer [29]. The biological activity of the same commercial AMH product as what was used in the current study was reported previously in in vitro studies using rat ovary organ culture [30], monkey ovarian follicle culture [4], and human endometrial stromal cell culture [31], as well as in in vivo studies of AMH effects on the hypothalamic-pituitary-gonadal axis via intracerebroventricular administration [14]. Besides recombinant human protein supplementation, overexpression of macaque AMH mediated by viral vectors could be performed in future studies using the current matrix-free follicle culture system.

In summary, the current study developed a molecular approach that now provides a tool to study the intraovarian/intrafollicular effects of AMH both in vitro and in vivo. This study also accentuates the critical local regulatory role of AMH during preantral follicle development in the primate ovary. Endogenous AMH production appears crucial for granulosa cell health and proliferation, and thus, preantral follicle survival and growth. Subsequent studies are ongoing, using the current experimental models with increased sample sizes, to investigate AMH-regulated follicular cell proliferation,

differentiation, and function during the antral follicle development in primates.

Supplementary data

Supplementary data are available at [BIOLRE](http://www.biolreprod.org) online. Table S1. Antibody table.

Acknowledgments

We are grateful for the assistance provided by members of the Division of Comparative Medicine, the Pathology Services Unit, the Surgical Services Unit, the Assisted Reproductive Technologies Support Core, the Endocrine Technology Support Core, the Histopathology-Morphology Research Core, the Imaging & Morphology Support Core, the Molecular & Cellular Biology Support Core, the Molecular Virology Support Core, and the Biostatistics and Bioinformatics Unit at ONPRC, OHSU. We appreciate Drs. Flor Sánchez and Sergio Romero at the Vrije Universiteit Brussel for their valuable expertise.

References

- Durlinger AL, Visser JA, Themmen AP. Regulation of ovarian function: the role of anti-Müllerian hormone. *Reproduction* 2002; 124:601–609.
- Baarends WM, Uilenbroek JT, Kramer P, Hoogerbrugge JW, van Leeuwen EC, Themmen AP, Grootegoed JA. Anti-müllerian hormone and anti-müllerian hormone type II receptor messenger ribonucleic acid expression in rat ovaries during postnatal development, the estrous cycle, and gonadotropin-induced follicle growth. *Endocrinology* 1995; 136:4951–4962.
- Xu J, Xu F, Letaw JH, Park BS, Searles RP, Ferguson BM. Anti-Müllerian hormone is produced heterogeneously in primate preantral follicles and is a potential biomarker for follicle growth and oocyte maturation in vitro. *J Assist Reprod Genet* 2016; 33:1665–1675.
- Xu J, Bishop CV, Lawson MS, Park BS, Xu F. Anti-Müllerian hormone promotes pre-antral follicle growth, but inhibits antral follicle maturation and dominant follicle selection in primates. *Hum Reprod* 2016; 31:1522–1530.
- Schmidt KL, Kryger-Baggesen N, Byskov AG, Andersen CY. Anti-Müllerian hormone initiates growth of human primordial follicles in vitro. *Mol Cell Endocrinol* 2005; 234:87–93.
- Eilso Nielsen M, Rasmussen IA, Fukuda M, Westergaard LG, Yding Andersen C. Concentrations of anti-Müllerian hormone in fluid from small human antral follicles show a negative correlation with CYP19 mRNA expression in the corresponding granulosa cells. *Mol Hum Reprod* 2010; 16:637–643.
- Andersen CY, Schmidt KT, Kristensen SG, Rosendahl M, Byskov AG, Ernst E. Concentrations of AMH and inhibin-B in relation to follicular diameter in normal human small antral follicles. *Hum Reprod* 2010; 25:1282–1287.
- Durlinger AL, Gruijters MJ, Kramer P, Karels B, Kumar TR, Matzuk MM, Rose UM, deJong FH, Uilenbroek JT, Grootegoed JA, Themmen AP. Anti-Müllerian hormone attenuates the effects of FSH on follicle development in the mouse ovary. *Endocrinology* 2001; 142:4891–4899.
- Rocha RM, Lima LF, Carvalho AA, Chaves RN, Bernuci MP, Rosa-e-Silva AC, Rodrigues AP, Campello CC, Figueiredo JR. Immunolocalization of the anti-Müllerian hormone (AMH) in caprine follicles and the effects of AMH on in vitro culture of caprine pre-antral follicles enclosed in ovarian tissue. *Reprod Dom Anim* 2016; 51:212–219.
- Xu M, Barrett SL, West-Farrell E, Kondapalli LA, Kiesewetter SE, Shea LD, Woodruff TK. In vitro grown human ovarian follicles from cancer patients support oocyte growth. *Hum Reprod* 2009; 24:2531–2540.
- Hayes E, Kushnir V, Ma X, Biswas A, Prizant H, Gleicher N, Sen A. Intracellular mechanism of Anti-Müllerian hormone (AMH) in regulation of follicular development. *Mol Cell Endocrinol* 2016; 433:56–65.
- Kano M, Sosulski AE, Zhang L, Saatcioglu HD, Wang D, Nagykerly N, Sabatini ME, Gao G, Donahoe PK, Pépin D. AMH/MIS as a contraceptive

- that protects the ovarian reserve during chemotherapy. *Proc Natl Acad Sci USA* 2017; **114**:E1688–E1697.
13. Campbell BK, Clinton M, Webb R. The role of anti-Müllerian hormone (AMH) during follicle development in a monovulatory species (Sheep). *Endocrinology* 2012; **153**:4533–4543.
 14. Cimino I, Casoni F, Liu X, Messina A, Parkash J, Jamin SP, Catteau-Jonard S, Collier F, Baroncini M, Dewailly D, Pigny P, Prescott M et al. Novel role for anti-Müllerian hormone in the regulation of GnRH neuron excitability and hormone secretion. *Nat Commun* 2016; **7**:10055.
 15. Xu J, Lawson MS, Yeoman RR, Molskness TA, Ting AY, Stouffer RL, Zelinski MB. Fibrin promotes development and function of macaque primary follicles during encapsulated three-dimensional culture. *Hum Reprod* 2013; **28**:2187–2200.
 16. Bishop CV, Hennebold JD, Kahl CA, Stouffer RL. Knockdown of progesterone receptor (PGR) in macaque granulosa cells disrupts ovulation and progesterone production. *Biol Reprod* 2016; **94**:109.
 17. Kennedy MA, Parks RJ. Adenovirus virion stability and the viral genome: size matters. *Mol Ther* 2009; **17**:1664–1666.
 18. Simpliciano C, Clark L, Asi B, Chu N, Mercado M, Diaz S, Goedert M, Mobed-Miremadi M. Cross-linked alginate film pore size determination using atomic force microscopy and validation using diffusivity determinations. *J Surf Eng Mater Adv Technol* 2013; **3**:1–12.
 19. Sánchez F, Romero S, Albuz FK, Smitz J. In vitro follicle growth under non-attachment conditions and decreased FSH levels reduces Lhcgr expression in cumulus cells and promotes oocyte developmental competence. *J Assist Reprod Genet* 2012; **29**:141–152.
 20. Majumdar SS, Winters SJ, Plant TM. Procedures for the isolation and culture of Sertoli cells from the testes of infant, juvenile, and adult rhesus monkeys (*Macaca mulatta*). *Biol Reprod* 1998; **58**:633–640.
 21. Xu J, Lawson MS, Yeoman RR, Pau KY, Barrett SL, Zelinski MB, Stouffer RL. Secondary follicle growth and oocyte maturation during encapsulated three-dimensional culture in rhesus monkeys: effects of gonadotrophins, oxygen and fetuin. *Hum Reprod* 2011; **26**:1061–1072.
 22. Bishop CV, Xu F, Xu J, Ting AY, Galbreath E, McGee WK, Zelinski MB, Hennebold JD, Cameron JL, Stouffer RL. Western-style diet, with and without chronic androgen treatment, alters the number, structure, and function of small antral follicles in ovaries of young adult monkeys. *Fertil Steril* 2016; **105**:1023–1034.
 23. Ghadami M, El-Demerdash E, Salama SA, Binhabazim AA, Archibong AE, Chen X, Ballard BR, Sairam MR, Al-Hendy A. Toward gene therapy of premature ovarian failure: intraovarian injection of adenovirus expressing human FSH receptor restores folliculogenesis in FSHR(-/-) FORKO mice. *Mol Hum Reprod* 2010; **16**:241–250.
 24. Durlinger AL, Kramer P, Karels B, de Jong FH, Uilenbroek JT, Groote-goed JA, Themmen AP. Control of primordial follicle recruitment by anti-Müllerian hormone in the mouse ovary. *Endocrinology* 1999; **140**:5789–5796.
 25. Kong HS, Kim SK, Lee J, Youm HW, Lee JR, Suh CS, Kim SH. Effect of exogenous anti-Müllerian hormone treatment on cryopreserved and transplanted mouse ovaries. *Reprod Sci* 2016; **23**:51–60.
 26. Bunz F, Dutriaux A, Lengauer C, Waldman T, Zhou S, Brown JP, Sedivy JM, Kinzler KW, Vogelstein B. Requirement for p53 and p21 to sustain G2 arrest after DNA damage. *Science* 1998; **282**:1497–1501.
 27. Wang TR, Yan J, Lu CL, Xia X, Yin TL, Zhi X, Zhu XH, Ding T, Hu WH, Guo HY, Li R, Yan LY et al. Human single follicle growth in vitro from cryopreserved ovarian tissue after slow freezing or vitrification. *Hum Reprod* 2016; **31**:763–773.
 28. McGee EA, Smith R, Spears N, Nachtigal MW, Ingraham H, Hsueh AJ. Müllerian inhibitory substance induces growth of rat preantral ovarian follicles. *Biol Reprod* 2001; **64**:293–298.
 29. di Clemente N, Jamin SP, Lugovskoy A, Carmillo P, Ehrenfels C, Picard JY, Whitty A, Josso N, Pepinsky RB, Cate RL. Processing of anti-Müllerian hormone regulates receptor activation by a mechanism distinct from TGF-beta. *Mol Endocrinol* 2010; **24**:2193–2206.
 30. Nilsson EE, Schindler R, Savenkova MI, Skinner MK. Inhibitory actions of anti-Müllerian Hormone (AMH) on ovarian primordial follicle assembly. *PLoS One* 2011; **6**:e20087.
 31. Wang J, Dicken C, Lustbader JW, Tortoriello DV. Evidence for a Müllerian-inhibiting substance autocrine/paracrine system in adult human endometrium. *Fertil Steril* 2009; **91**:1195–1203.